Spin-dependent electronic transport through a porphyrin ring ligating an Fe(II) atom: An *ab initio* study

Yunqing Chen, Alexander Prociuk, Trilisa Perrine, and Barry D. Dunietz*
Department of Chemistry, University of Michigan, Ann Arbor, Michigan 48109, USA
(Received 1 May 2006; revised manuscript received 27 August 2006; published 18 December 2006)

Conductance calculations employing density functional theory methodology and Landauer formalism predict that a ligated iron atom can be used as a switching device. The iron atom is ligated in our models by a porphyrin molecule. The iron-porphyrin molecular device is shown to lose more than 66% of its conductance by shifting from the low spin coupling state to excited spin states. Further reduction is also correlated with a mechanical distortion of the porphyrin plane. Both the distortions and spin transitions are fast processes that can be invoked by manipulating the iron's ligation scheme through the axial ligands.

DOI: 10.1103/PhysRevB.74.245320 PACS number(s): 73.23.−b, 72.25.−b, 73.40.Sx, 31.15.Ar

INTRODUCTION

Recently a surge in the use of experimental techniques to fabricate electronic devices based on single molecules has been reported.[1–5] Such devices are possible due to the ability to manipulate the conducting matter at the atomic level. Molecular wires have been shown not to conduct as simple ohmic resistors, but rather to possess a conductance spectra which depends on their electronic structures.[3,4,6,7] One of the fundamental challenges faced by molecular electronics research is to identify molecules or nanomaterials with several accessible metastable states which greatly differ in their electrical conductance. When the transition between these states can be manipulated, such materials may be used as molecular devices, switches, or sensors. Several experimental successes have been reported. These include the rotaxane based Stoddart-Heath[1] (SH) and the nitroamine based Tour-Reed[2] molecular switches. Computational studies of the conductance employing Green function analysis on related models have provided possible insight into the mechanism of these devices.[8,9] Even more successful has been the employment of conductance changes induced by the presence of analyte molecules for sensing applications.[10–15]

The related field of spintronics utilizes the spin coordinate as an additional variable affecting conductance of materials sandwiched between layers of ferromagnetic material.[16,17] Spin polarized transport through molecular layers immersed between two magnetic layers has been demonstrated for systems involving carbon nanotubes,[18] other organic π conjugated systems,[19,20] molecular bridges,[21] and molecular tunnel junctions.[22] In these experiments large dependence on an applied magnetic field of the electronic transport has been demonstrated. Spin valve effects, where the transport property of the molecular wire sandwiched between two magnetic units (for example, Ni atom clusters), have been studied computationally for a carbon chain[23] and dithiolated benzene ring.[24,25] More recently, computational studies on related molecular magnetoresistors, where dithiolated benzene sandwiched between nickel contacts,[26] iron contacts,[27] and tricene within nickel[28] were shown to possess conductance controllable by a magnetic field. Tunneling current through a single-molecule magnet metal in a STM system was studied theoretically.[29] In these studies, different transmission properties were demonstrated for the leads parallel and antiparallel spin alignment cases. Other recent studies report spin polarized transmission, where the transmission depends on the spin coupling state of the conducting device. These studies focus on spin polarized transport through polyphenoxyl radical molecule[30] and dicobaltcene based junctions.[31] In these applications a magnetic field can be utilized to switch between the different molecular states. The ability to introduce active spins into the device rather than the leads is further studied here by considering a ligated porphyrin molecule.

In this paper we report calculated conductance changes based on chemical changes of a molecular device consisting of a single porphyrin ring ligating a Fe(II) metal atom center. Previously, locating a single porphyrin between gold atom wires was achieved by manipulating single gold atoms with a STM tip.[32] In addition, an array of porphyrin rings was shown to perform as a good conductor.[33] Other porphyrin containing devices were engineered as well.[34] For example, the ability to control electron transfer within arrays of donor-acceptor sites was demonstrated on adlayers of porphyrin-perylene systems. In optoelectronics the conductivity of porphyrin-perylene arrays can be varied by optically inducing charge transfer.[35,36]

The conductance variances suggested from our calculations are based on changes in the spin state of the ligated iron atom. These changes can be triggered by a combination of manipulating the ligation scheme and application of magnetic fields. The role of a metal center in a molecular device to enhance its functionality was demonstrated before. For example, a self-assembled layer of porphyrin molecules can functionalize a semiconductor nanowire to perform as a data-storage device only when chelated by Co(II) atoms.[34] On another system, computational studies showed that chelating metals drastically change conductivity of crown ethers suggesting another setup for a metal recognition or an electronic switching device[37] and even more related is the spin-dependent transmission through the tunnel junction based on dicobaltcene molecular devices.[31]

METHOD AND MODEL

Most molecular conductivity calculations are based on the Landauer description of noninteracting scattering electrons.[38]

In this approach conductivity is evaluated by integration over quantum mechanical transmission

$$I(V) = e/h \int T(E,V)[f_l(E,\mu_l) - f_r(E,\mu_r)]dE, \qquad (1)$$

where T is the (molecular) transmission function and f_l and f_r are the Fermi distributions of the leads. The transmission function peaks at molecular electronic levels due to scattering events through the conductor.

In order to treat the infinite system an extended molecular model is employed. In this picture the system is subdivided into three parts, i.e., the left and right electrodes and the molecular scattering region. Therefore the electronic integrals matrices (Hamiltonian and overlap matrices) are divided into 3×3 sections. This is performed for each spin component, separately. Therefore, the overall conductivity is a result of summing over the spin coordinate (σ):

$$I(V) = \sum_{\sigma=\alpha,\beta} I^{\sigma}(V). \qquad (2)$$

The (spin dependent) transmission is expressed by

$$T^{\sigma}_{ab}(E,V) = \mathrm{tr}[G^{R,\sigma}_c \Gamma^{\sigma}_l G^{A,\sigma}_c \Gamma^{\sigma}_r], \qquad (3)$$

where G^{σ}_c is the molecule Green's function and Γ is the broadening function. The broadening function is related to the coupling of the conductor to the contacts, which is described through the self-energies (SEs).[7,39–41] The SEs are a result of projecting the bulk green function

$$g_l(E) = (ES_l - H_l)^{-1}, \qquad (4)$$

on the device by the electronic coupling Hamiltonian (H_{lc}) and overlap (S_{lc}) matrices:

$$\Sigma^{\sigma}_l = (H^{\sigma}_{cl} - ES_{cl}) g_l (H^{\sigma}_{lc} - ES_{lc}). \qquad (5)$$

Note, the gold bulk is kept spin restricted. Future research will study the spin-dependent transport with ferromagnetic metals where also the bulk GF is spin dependent. In addition, since no spin-flip effects are included in the model, the two spin channels are assumed to be independent and therefore are added to express the overall conductance.

The bulk GF can further be simplified by assuming it to be constant of the energy. This constitutes the wide band limit (WBL) approximation. In this approximation, the bulk can be assumed to be dominated by the S band. This translates the bulk's GF ($g_{l,r}$) to be a simple constant factor. Alternatively, a more accurate (and complex) representation of the bulk can be achieved by solving efficiently[42] a tight-binding (TB) model of the bulk at every energy. Here, the TB model is employed with calculated electronic parameters from a separate electronic structure calculation of the considered bulk (DFT-based TB model). These two levels of bulk representation are employed and the corresponding evaluated transmission function is compared below.

Following the calculation of the transmission, the conductance $[g(V)]$ is evaluated from the $I(V)$ relation given above [Eq. (1)] with the following assumptions. At low temperatures it is appropriate to approximate the Fermi distributions by step functions. In addition, the potential drop within the molecule is neglected: Thus, the conductance is proportional to the transmittance as $g(V) = \frac{\partial I}{\partial V} \approx (e^2/h)1/2[T(\mu_1) + T(\mu_2)]$, where $\mu_{1,2} = E_f \mp 1/2eV$ and E_f is the lead's Fermi energy (FE). The above approach has been introduced and discussed in detail by others[7,41,43–46] and was shown to reproduce the shape of several experimental conductance curves.[43,46]

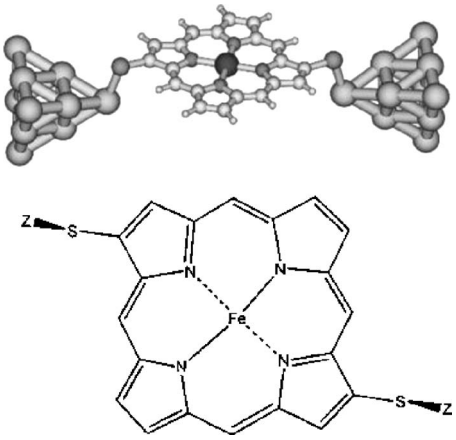

FIG. 1. The modeled molecular device consists of a porphyrin molecule bonded to two gold atoms through thiolate atoms. The lower inset describes the molecular plane of the ligated porphyrin species. In the upper part the porphyrin is thiol-bonded to two gold tips, in a tablelike conformation.

The quantum electronic transmission of a porphyrin ring ligating an Fe(II) atom has been evaluated at different spin states. In Fig. 1, the molecular model used in the calculation is depicted. We model a molecular junction composed of a single porphyrin bonded to two gold tips through thiolate groups. The geometries of the molecule and the two thiolate bonded gold atoms were fully optimized for the different spin states. We have also considered the porphyrin ring without the ligated iron center. For the conductivity calculation, these geometries are complemented by a larger gold cluster model in order to simulate better the gold tip contacts. This cluster model consists of the three outermost layers of a perfect tip where a Au(111) plane is assumed with 2.86 Å as the crystal parameter (total of 10 Au atoms shown in the left inset). All electronic structure calculations were performed at the density functional level employing the B3LYP functional[47,48] with the sophisticated LANL2DZ basis set[49] (the electronic structure software used is Qchem[50]).

The bulk gold FE is −5.1 eV, our highest occupied MOs have a slightly higher energy due to the use of a truncated cluster model. Therefore the FE has been set to −5.0 eV. The transmission has been calculated for the porphyrin at the different spin and ligation schemes. The bulk is represented either at the WBL level or by an explicit DFT-TB model calculation for the bulk which is repeated at every energy. The TB parameters have been extracted from a separate bulk calculation involving four to seven layers, where convergence of the calculated transmission is confirmed for using a bulk model consisting of six or seven layers.

RESULTS AND DISCUSSION

The transmission function due to the broadened porphyrin molecular orbitals (MOs) is provided in Fig. 2, where we

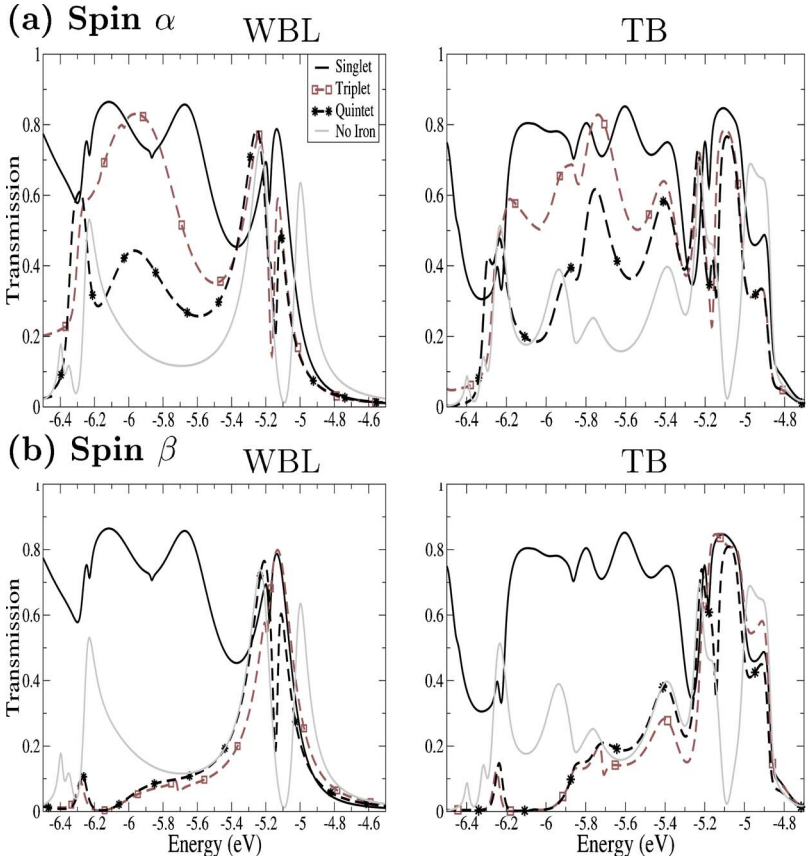

FIG. 2. (Color online) The different transmission functions calculated by employing the WBL approximation for representing the bulk (a) and a first-principles TB model (b) at the different spin coupling states of the iron-porphyrin system (four ligation scheme). The conductance includes different contributions from the spin α and β channels for the excited spin coupling states.

include the transmission through the unligated system and the different spin states of the ligated system. In the upper panel the transmission corresponding to the α spin orbitals, where the β transmissions are provided in the lower panel. In the left side of each panel the WBL representation of the bulk is used and in the right side of the panel the TB approach is implemented. We find that for all considered systems transmission through the unoccupied orbitals is vanishing. Therefore we focus our analysis only on the relevant energy region of the frontier occupied orbitals. This corresponds to a region of about 1.5 eV below −5.0 eV. In the next subsections we describe the transmission properties of the iron-ligated and unligated porphyrin. We begin by describing the effect of the iron center on the porphyrin transmission. We then focus on the spin dependent transmission of the iron ligated system and the effect of axial ligation on the transmission properties. The origin of the described transmission trends are then analyzed and explained by considering the relevant orbitals and electronic densities of states. Finally, the consequence of adding axial ligands on transmission are studied. Axial ligation influence on the relative energetics of the different spin coupling states is a well studied effect.

Iron center effect on transmission through a porphyrin. We begin our investigation by focusing on the effect of the iron center on the transmission of a porphyrin ring bonded between two gold tips. Therefore, we focus first on comparing the transmission through the unligated system and the corresponding singlet state of the iron (II) ligated system. We note that the transmission due to the first two MOs is comparable for all considered systems. These are the highest occupied orbitals of the porphyrin system and are located in energy close to −5.0 eV for all systems. The full list of the orbital assignments and energies is provided in Fig. 5 and Table I and is discussed in detail below. We find that the transmission due to lower lying orbitals is dramatically varied by the presence of the iron center. The interband gap is shown to decrease substantially upon the ligation of the iron atom, where this gap decreases from 1.0 eV for the free porphyrin to 0.6 eV for the iron-porphyrin or from 0.65 to 0.29 eV when bonded to the gold tips. A careful analysis of the transmission function, however, implies a complex effect of the iron center. As will be discussed in detail below, the presence of the iron can also lead to a degradation of the transmission as observed for the transmission of β spin channel at the higher spin coupling states. The dependence of the transmission on the spin state is analyzed in detail below.

Spin-dependent transmission of the four ligated system. Here we focus on comparing the transmission properties of the four ligated system at the different spin coupling states available due to the iron center. Several observed trends should be highlighted. The singlet appears to possess the best transmission properties as it shows the widest broadening of the transmission peak near the FE (highest occupied porphyrin MO). Furthermore, the broadening of the β spin transmission peaks of the spin excited states at the FE are narrower than the corresponding spin α. Thus it appears that the β electron spin transmission channel is turned off at energy values near the Fermi level. Interestingly, the narrowest β peak is observed for the triplet case and the quintet is only

TABLE I. Porphyrin MO energies at the different considered systems. Also provided are the nonthiolated porphyrin and iron-porphyrin energies. The sequence adopted by the thiol functionalized singlet FeP molecule is used in defining the order of the rows in the table. The D_{4h} notation is used for all systems to allow easy reference to the well studied iron-porphyrin electronic structure.

Orbital type	Free		Thiolated-gold tips					
	P	FeP	P	FeP	Triplet		Quintet	
a_{1u}/a_{2u}	−5.16	−5.26	−4.99	−5.06	−5.11	−5.07	−5.11	−5.09
	−5.41	−5.29	−5.19	−5.18	−5.18	−5.20	−5.19	−5.16
$1e_g$ (parallel)	−6.35	−5.94	−5.81	−5.47	−5.59	−5.76	−5.65	−5.73
$b_{2u}[+a_{2u}]$	−6.51	−6.64	−5.98	−5.85	−5.88	−5.87	−5.87	−5.85
$2e_g$ (perpendicular)	−7.18	−5.94	−6.26	−5.87	−6.17	−6.78	−6.44	−6.70
$b_{2u}[-a_{2u}]$	−7.23	−7.05	−6.39	−6.71	−6.71	−6.71	−6.70	−6.66
AuS[+Fe]			−6.31	−6.18	−6.22	−6.24	−6.22	−6.22
			−6.32	−6.21	−6.27	−6.25	−6.30	−6.24
				−6.25	−6.61			

slightly wider (still both are much narrower than the α channels).

These trends are observed at both levels of bulk representations with, however, several differences. The more explicit TB description exhibits features absent from the results obtained with the WBL bulk description. At the WBL bulk description the different curves exhibit some strong energy localization effects. These are artifacts, which are due to the simplified cluster model of the bulk electrode material in this level. However, both levels of theory, as mentioned above, demonstrate the same overall trend where the excited spin state channels exhibit lowered transmission with spin excitation. This is even more apparent when the conductance plots at the two levels of theory are compared. We associate these trends to electronic effects induced by the iron atom as is analyzed below by considering the relevant frontier orbitals in the different spin coupling schemes.

The general trends underlying the variance of the transmission are evident by comparing the different conductance curves at moderate voltage bias. In Fig. 3 the conductance as a function of the voltage bias for the different spin states is sketched. Both possible spin channels at excited spin coupling states are provided. The conductance is evaluated as described above. The conductivity comparisons should apply a factor of two for the singlet and involve the sum of the two channels for the triplet and quintet states separately. The superiority of the singlet state as a conductor is well demonstrated and is emphasized at small and moderate voltage bias. Similar observations are obtained at both levels of bulk representation.

It is important to note that the variance of the transmission is not merely a consequence of the spin excitation leading to change of the orbital population and therefore to changes in transmission. This is easily verified by noting that the transmission of the porphyrin molecule optimized at a triplet spin coupling is very similar to the transmission of the "correct" singlet spin coupling optimization. The triplet transmission in the absence of an iron center is compared to the singlet base transmission in Fig. 4(a), where the spin polarization in the triplet state is shown to be negligible and very similar to the singlet. Furthermore, it is also verified that the (minor) structural relaxations induced by the spin excitation are not

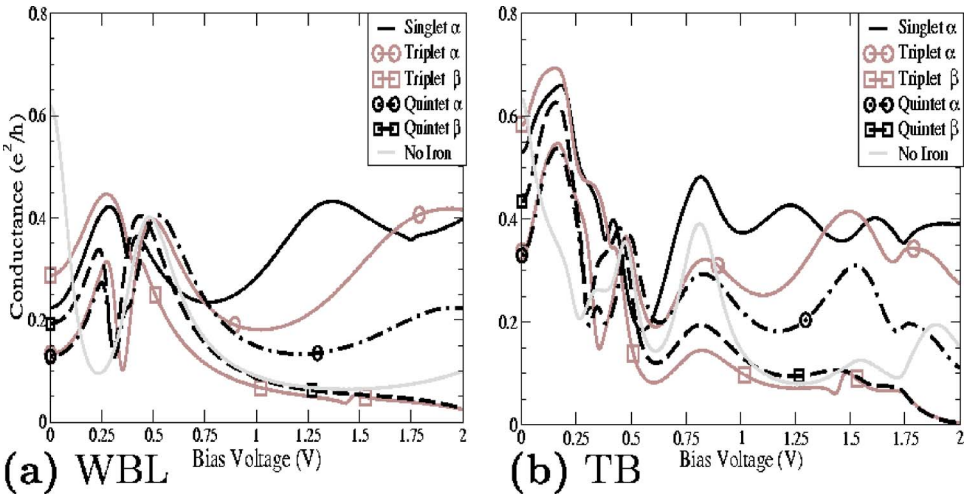

FIG. 3. (Color online) The different conductance curves of the four ligated system calculated at the WBL (left side) and TB (right) levels for representing the bulk.

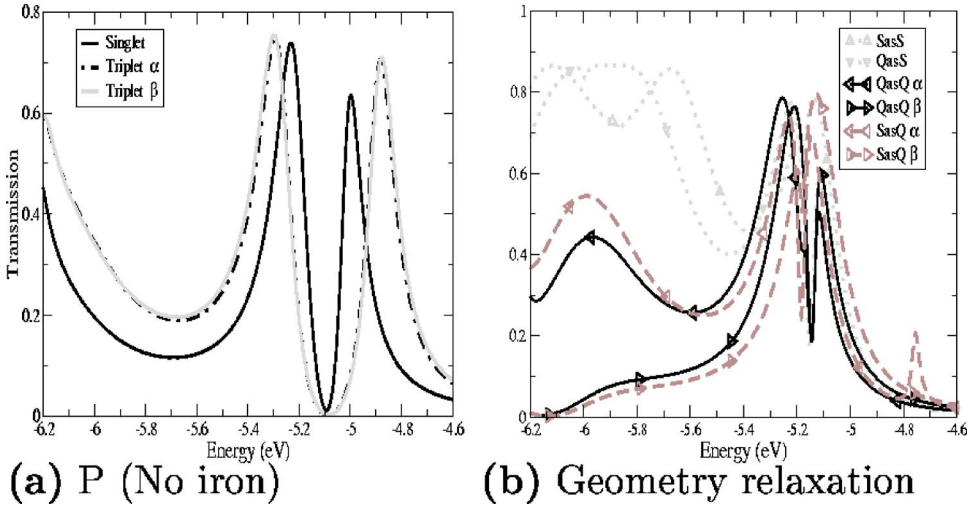

FIG. 4. (Color online) The origin of the transmission dependence on the spin coupling state is analyzed. The effect on transmission is negligible due to (a) the spin coupling scheme in the absence of the iron center and (b) the geometry relaxation induced due to the spin coupling scheme in the presence of the iron center. Therefore, the electronic relaxation induced by the spin coupling state induced by the iron center is the major factor responsible for the strong dependence of the transmission on the spin state.

responsible for the noted spin dependent transmission. This is verified by using the singlet geometry in a quintet calculation or in the other direction where the quintet geometry is used in a singlet calculation. This is noted, respectively, QasS and SasQ in Fig. 4(b), where it is shown that the observed transmission trends are *not* rooted in the structural changes induced by the spin-coupling scheme. Therefore, it is rather the changes in the electronic density introduced through the iron center at different spin coupling states, which underlies these transmission trends. The important role of the iron atom in leading to spin dependent transmission is analyzed in detail below by considering the explicit relaxation effect on the orbitals due to the varying spin coupling state.

Iron's electronic density role in the spin dependent transmission. The effect of the iron center on the porphyrin transmission has been shown to play a complex role. This suggests the possibility for engineering different devices for applications ranging from metal recognition, molecular switches, and spin filters. A fundamental understanding of the effects underlying these observations is an important step in this direction. This is achieved below by analyzing in detail the transmission functions and relating the observed trends to the relevant molecular orbitals.

In Table I we tabulate the porphyrin orbital energies at the different spin states and upon binding to the thiolated gold tips through the sulfur atom. The orbitals are listed in the order adopted in the singlet form with the gold tips. We also "borrow" the D_{4h} symbols for associating these orbitals to the familiar notation of the Fe-porphyrin species. The first two transmission peaks are related to the two highest occupied porphyrin molecular orbitals. These orbitals involve a complete π ring system. It is observed that these orbitals transmit quite uniformly across the different considered cases. The strong difference of the transmission is evident due to combined broadening effects of these first band orbitals with the next orbitals. It is interesting to note that the splitting of the first band is maximal for the porphyrin lacking the iron center, which explains the almost vanishing transmission between the two orbitals at around −5.1 eV. The iron-porphyrin systems, on the other hand, all feature more efficient broadening effects in the −5.0 to −5.2 eV energy region.

Considering the next lower lying occupied orbitals, we find that the functionalization of the porphyrin ring by the gold tips breaks the degeneracy of the second band of iron-porphyrin orbitals (the e_g orbitals). These π orbitals involve a diagonal connecting β-porphyrin ring sites located across from each other. The more stabilized orbital is oriented along the diagonal which is perpendicular to the line connecting the two tips (noted perpendicular in the table). It is, therefore, expected to contribute less to conductance through the porphyrin.

The orbital with higher energy, however, is found to be functionalized along the line connecting the two tips and is shown to affect substantially the transmission pattern (this is noted parallel in the table). The splitting of the second band locates this orbital closest in energy to the first band orbitals in the singlet spin coupling case (this energy gap is referred to above in comparing this gap to the noniron system separation). This energy gap between the two bands for the different spin coupling states can be extracted from the orbital energies table by the difference between the values in the second and third rows. It is observed that for the singlet this difference is the smallest and that it gradually increases with the spin excitation. Even more important is the increase of this value for the β case when compared to the α spin for either the triplet and quintet spin multiplicities. This underlies the more efficient transmission observed for the singlet state and the α spin channels at the energy region beyond the first band (−5.4 to −5.9 eV). We consider, next, the transmission through the remaining porphyrin orbitals which are related to the 2–3 first bands. This trend of varying contribution of the Fe AOs is also well demonstrated in Fig. 5, where all orbitals are drawn with the same isosurface value.

The next orbital listed in the table is also oriented along the "correct" diagonal. It can be described as a superposition of the free iron-porphyrin (FeP) a_{2u} and b_{2u} orbitals. An illustration of this orbital is provided in Fig. 5 as well. This orbital is shown to be further shifted to lower energies with higher spin excitations and even further down for the β spin orbital sets. This shift is also found to correlate well with the decreasing contribution of the iron's AOs to this orbital. It is found that the PDOS on the iron AOs of this MO is decreasing with the spin excitation or when considering the *beta*

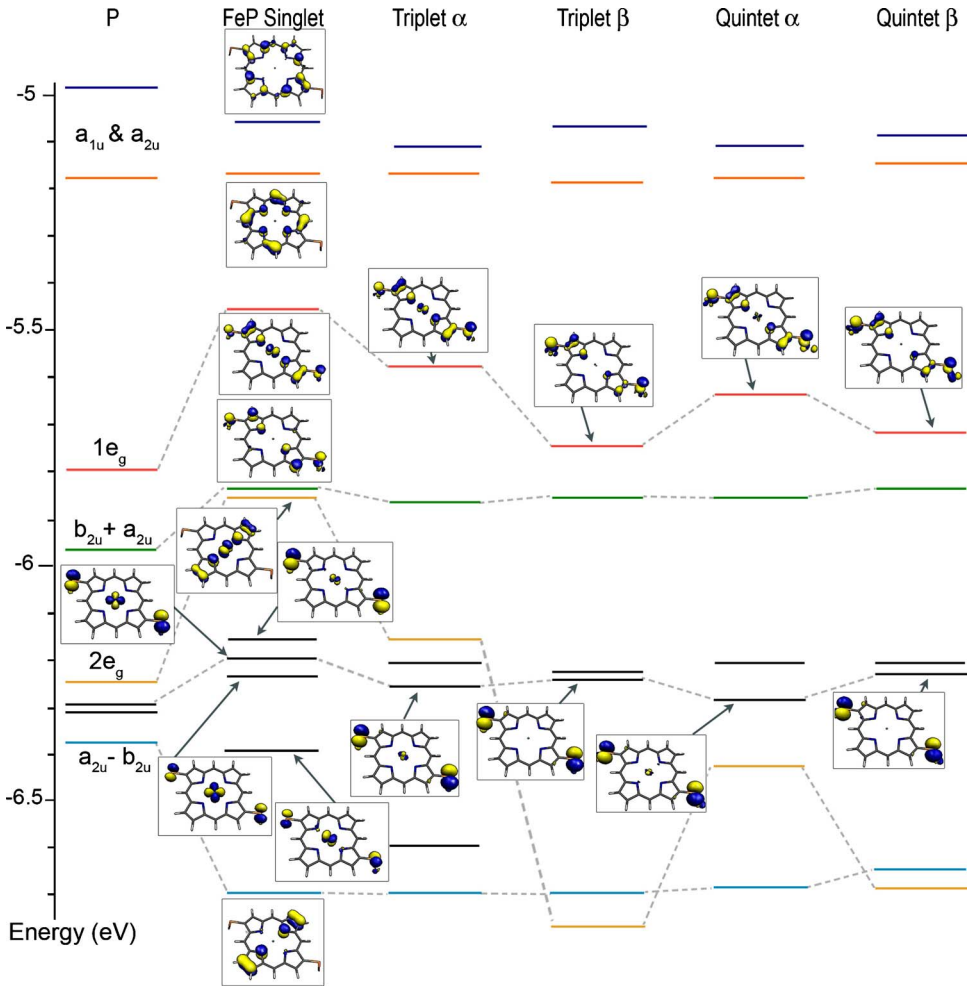

FIG. 5. (Color online) Porphyrin orbital diagram for the free molecule and FeP at the different spin coupling states with the gold tip functionalization. Also included in the first two columns are, respectively, the nonthiol functionalized porphyrin and singlet FeP orbitals. Of high interest is the apparent changing contribution of the Fe AOs to the e_g porphyrin and AuS orbitals. All unlabeled (black lines) states are of Au[+Fe] character. Pure Fe orbitals have been omitted.

spin orbital. We list the relative contribution of the Fe's AOs by considering the percentage of projected DOS on the iron from the total DOS of the full molecule in Table II. This analysis is performed on the MOs of the cluster model.

Other orbitals listed in Table II in the relevant energy region are found to present the same trends. The other orbitals which are considered here involve the other combination $(b_{2u}-a_{2u})$ of these porphyrin orbitals, the lower lying e_g orbital and orbitals which are dominated by the AuS contribution (nonporphyrin orbitals). These orbitals are also listed in the remaining rows in the orbitals table. It is noted that the transmission due to these orbitals is highly dependent on the relative weight of the Fe atomic orbitals. The β spin orbitals have substantially reduced contribution from the iron compared to the corresponding α orbitals. This is correlated well with much reduced transmission at the relevant energy region. The relation of decreasing transmission and iron participation is also noted for the singlet, triplet, and quintet spin coupled states, where the iron participation in the hybridization of these MOs is essential to allow high transport properties of these (diagonal) orbitals. Namely, the transmission is dependent on the iron as a linking unit for orbitals which are not delocalized around the ring.

Effect of the axial ligation on transmission. The energy splitting due to the spin state of the FeP molecules depends on the axial ligands. The singlet spin state becomes the low-

TABLE II. The iron contribution to the molecular orbitals presenting strong spin dependence transmission. The percentage of the iron PDOS to the total DOS related to each orbital is listed. The values in parentheses are the MO energies.

Orbital	FeP Singlet	FeP Triplet		FeP Quintet	
1*eg*	(−5.47) 17%	(−5.58) 6.5%	(−5.76) 1.2%	(−5.65) 1.3%	(−5.73) 1.2%
2*eg*	(−5.87) 44%	(−6.17) 24%	(−6.78) 2.9%	(−6.44) 5.6%	(−6.70) 2.8%
AuS+Fe	(−6.17) 5.7%	(−6.22) 1.1%	(−6.24) 0.18%	(−6.22) 0.25%	(−6.22) 0.22%
	(−6.21) 33%	(−6.27) 4.0%	(−6.25) 0.61%	(−6.30) 2.4%	(−6.24) 0.69%
	(−6.25) 63%	(−6.61) 19%			

TABLE III. Relative energies of the Fe(II) ion dependence on the spin coupling state within different porphyrin-based ligation. The geometry optimizations involving the single gold atom are included as well as the single point calculations involving the tip models. Energies are in Kcal/mol relative to the singlet coupling state.

System	Triplet	Quintet
	No gold-thiol	
FeII	−52.8	−91.8
FeP	−32.4	−17.4
FeP-Im	−5.5	−2.5
CO-FeP-Im	39.1	41.2
	Single gold-thiol optimization	
FeP	−31.6	−22.2
FeP-Im	−3.55	−3.51
CO-FeP-Im	29.1	57.1
	Gold-tip-thiol SP	
FeP	−42.0	−35.4

est only with two axial ligands present (for example a histidine group in heme proteins and an additional molecule on the opposite site). In the singlet spin state planarity of the porphyrin ring is preferred. On the other hand, when only a single axial ligand is present distortion of the FeP plane is well known to occur,[51,52] where excited spin coupling states become more stabilized. Therefore, transition to a domed structure can be provoked, for example, from a fully six ligated system by dissociating the other axial ligand (CO, O_2, or N_2).[53] Previous DFT studies have been shown to reproduce well this doming mode.[54–56] These energetics are also summarized in Table III, where the axial ligation dependence energetics of the thiol-gold functionalized porphyrin system is summarized. In the table the singlet stability is demonstrated to be achieved only at the full six ligation scheme, as expected from the discussion above. Next we, therefore, consider the effect of the presence of axial ligands on the transmission curves and discuss its possible utilization.

We consider, first, the effect of the axial ligation on the conductance at the same spin coupling state. In Fig. 6 we provide a scheme which describes the considered five and six ligated systems below. The axial ligation includes a CO molecule as the second axial ligand, where the histidine group is the fifth ligand (first axial ligand). Our calculations show that the axial ligation does not eliminate the transmission variances among the different spin states. Namely, the transmission of the six ligated singlet system resembles that of the four ligated singlet case. Similarly we find for the quintet case that the five ligated and four ligated systems present similar transmission curves. The axial ligation in porphyrin is known to add orbitals which are oriented perpendicular to the plane, these orbitals do not seem to affect transmission through the plane of the porphyrin. The corresponding $T(E)$ curves are provided in Fig. 7(a).

This, therefore, suggests the ability to promote a scheme inducing spin-polarized current by a chemical manipulation. This can be exploited practically, for example, to act as a sensor, where a substantial increase in conductance can indicate the presence of gas phase molecules as CO, N_2 and O_2. This is further demonstrated below by comparing directly the conductivity plots of the five ligated system to the six ligated system, where the effect of the additional CO ligand is emphasized. Certainly, the study of the differential response to specific molecules is a desired and planned research direction that may suggest an even more selective sensor.

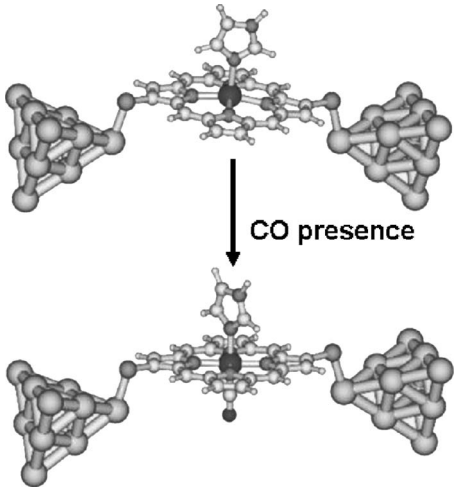

FIG. 6. The considered change in the axial ligation from a five ligated system to a six ligated system, where an addition of a CO ligand as the second axial ligand is illustrated.

Spin current. The conductivity of the different spin channels of the quintet five-ligated system and the singlet of the six-ligated system are depicted in Fig. 7(b). Also provided in the figure is the direct comparison of the summed conductivity plots (involving the sum over the spin channels at each state). First we note again, that both the WBL and the TB models of the bulk lead to very similar conductivity plots. Second, it is demonstrated that for the spin-excited state the current is dominated by the spin α transport, while the bulk material is spin unpolarized. It is apparent that the sum of the two spin variables is comparable (slightly below) to a single singlet spin channel. This underlies the over-factor of two drop of conductance predicted for the spin-excited state. The difference in efficiency of electron-transport demonstrated for the different spin channels can be exploited to generate spin polarized currents defining a spin valve or a spin filter, where the electron spin sites are within the device. Therefore, it is essential to study the same effect, when the electrodes are a ferromagnetic material.

CONCLUSION

To conclude, we have studied the structure-function relations of ligated porphyrin by a metal atom employed as molecular devices. First, large changes of the organic porphyrin transmission due to ligation of the ring by an iron center are noted. The strong ligation of metals by porphyrin and the induced dramatic effect on transmission, therefore, imply the possibility of using porphyrin-based devices for metal recognition applications. Furthermore, the spin dependent trans-

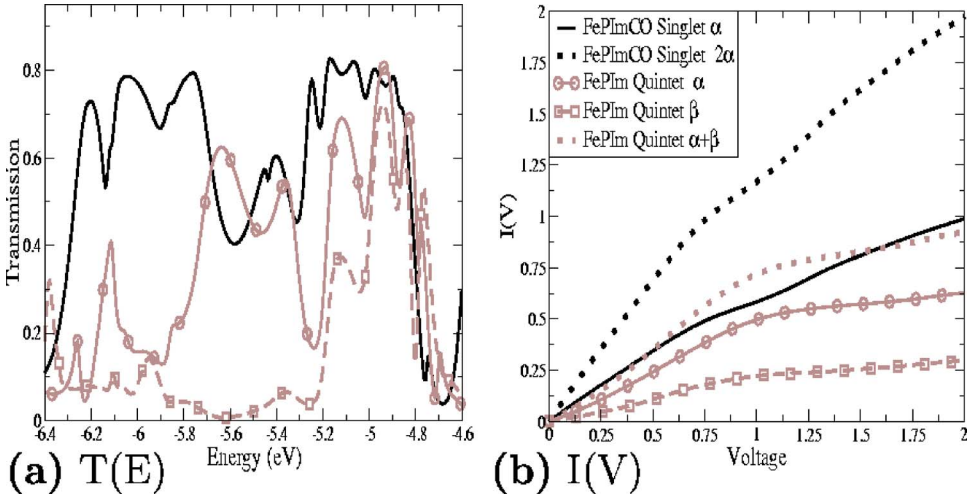

FIG. 7. (Color online) Effects of axial ligation on the transmission (a) and conductivity (b). The quintet state of the five ligated system (FePIm) and the singlet six ligated system (FePImCO) are compared.

mission induced upon iron center ligation suggests an additional array of applications. The spin state of the ligated porphyrin system can be controlled by a combination of utilizing magnetic fields and manipulation of the axial ligation scheme. The axial ligation determines the preferred spin state of this system. In this study, strong variance of the transmission pattern upon change of the spin coupling state is predicted. Therefore, changes in the spin coupling state that are induced by changes in the axial ligation of FeP molecules are predicted to lead to large changes of the conductance. This implies the applicability of the porphyrin-based system to function as a sensing device. This device responds to the presence of chemical species which interact with the porphyrin system as axial ligands.

The spin-coupling hierarchy of the conductance is shown to obey the singlet, triplet, and quintet sequence. The conductance drops are observed upon spin state excitation at low voltage bias values of over 0.1 and become more dramatic at the still modest bias of 0.5 and 1.0 V. As a final note, the large changes of the transmission are associated with strong spin polarization at the spin excited states, where the spin α transmission dominates. This strong bias of the spin-dependent transport can lead to development of spin filters or spin valves. In this study the spin polarization site is within the device as opposed to the majority of current spintronics related applications.

Additional research is planned to gain insight on the conductance properties of different ligated porphyrin systems. This can assist in determining the optimal ligated porphyrin molecular device and to distinguish the specific response of the conductance to different ligating molecules. These investigations may explore related devices consisting of different porphyrin derivatives and ligation of different metal ions. It is also of interest to study the same effects with ferromagnetic bulk materials, where it is predicted that the spin-dependent transmission of FeP may be further utilized and emphasized.

ACKNOWLEDGMENTS

B.D.D. acknowledges the University of Michigan for support and Joshua Schreir and Roi Baer for useful discussions.

*Electronic address: bdunietz@umich.edu

[1] C. P. Collier, E. W. Wong, M. Belohradsky, F. M. Raymo, J. F. Stoddart, P. J. Kuekes, R. S. Williams, and J. R. Heath, Science **285**, 391 (1999).
[2] J. Chen, M. A. Reed, A. M. Rawlett, and J. M. Tour, Science **286**, 1550 (1999).
[3] J. Park *et al.*, Nature (London) **417**, 722 (2002).
[4] W. J. Liang, M. Shores, M. P. Bockrath, J. R. Long, and H. Park, Nature (London) **417**, 725 (2002).
[5] M. C. Hersam and R. G. Reifenberger, Mater. Res. Bull. **29**, 385 (2004).
[6] M. A. Reed, C. Zhou, C. J. Muller, T. P. Burgin, and J. M. Tour, Science **278**, 252 (1997).
[7] W. Tian, S. Datta, S. Hong, R. Reifenberger, J. I. Henderson, and C. P. Kubiak, J. Chem. Phys. **109**, 2874 (1998).
[8] J. M. Seminario, A. G. Zacarias, and J. M. Tour, J. Am. Chem. Soc. **122**, 3015 (2000).
[9] Y. H. Kim, S. S. Jang, Y. H. Jang, and William A. Goddard III, Phys. Rev. Lett. **94**, 156801 (2005).
[10] H. Wohltjen and A. W. Snow, Anal. Chem. **70**, 2856 (1998).
[11] H. L. Zhang, S. D. Evans, J. R. Henderson, R. E. Miles, and T. H. Shen, Nanotechnology **13**, 439 (2002).
[12] Q. Y. Cai and E. T. Zellers, Anal. Chem. **74**, 3533 (2002).
[13] N. Cioffi, I. Farella, L. Torsi, A. Valentini, and A. Tafuri, Sens. Actuators B **84**, 49 (2002).
[14] L. Ruangchuay, A. Sirivat, and J. Schwank, Synth. Met. **140**, 15 (2004).
[15] J. Jang, M. Chang, and H. Yoon, Ann. Math. **17**, 1616 (2005).
[16] M. Johnson and R. H. Silsbee, Phys. Rev. Lett. **55**, 1790 (1985).
[17] S. A. Wolf, D. D. Awschalom, R. A. Buhrman, J. M. Daughton, S. von Molnar, M. L. Roukes, A. Y. Chtchelkanova, and D. M. Treger, Science **294**, 1488 (2001).

[18] K. Tsukagoshi, B. W. Alphenaar, and H. Ago, Nature (London) **401**, 572 (1999).
[19] Z. H. Xiong, D. Wu, Z. Valy Vardeny, and J. Shi, Nature (London) **427**, 821 (2004).
[20] V. Dediu, M. Murgia, F. C. Matacotta, C. Tiliani, and S. Barbanera, Solid State Commun. **122**, 181 (2002).
[21] S. Ouyang and D. D. Awschalom, Science **301**, 1074 (2003).
[22] J. R. Petta, S. K. Slater, and D. C. Ralph, Phys. Rev. Lett. **93**, 136601 (2004).
[23] R. Pati, M. Mailman, L. Senapati, P. M. Ajayan, S. D. Mahanti, and S. K. Nayak, Phys. Rev. B **68**, 014412 (2003).
[24] E. G. Emberly and G. Kirczenow, Chem. Phys. **281**, 311 (2002).
[25] R. Pati, L. Senapati, P. M. Ajayan, and S. K. Nayak, Phys. Rev. B **68**, 100407(R) (2003).
[26] D. Waldron, P. Haney, B. Larade, A. MacDonald, and H. Guo, Phys. Rev. Lett. **96**, 166804 (2006).
[27] H. Dalgleish and G. Kirczenow, Phys. Rev. B **72**, 184407 (2005).
[28] A. R. Rocha, V. M. Garcia-Suarez, S. W. Bailey, C. J. Lambert, J. Ferrer, and S. Sanvito, Nat. Mater. **4**, 335 (2005).
[29] G. H. Kim and T. S. Kim, Phys. Rev. Lett. **92**, 137203 (2004).
[30] K. Tagami and M. Tsukada, J. Phys. Chem. B **108**, 6441 (2004).
[31] R. Liu, S.-H. Ke, H. U. Baranger, and W. Yang, Nano Lett. **5**, 1959 (2005).
[32] G. V. Nazin, X. H. Qiu, and W. Ho, Science **302**, 77 (2003).
[33] D. H. Yoon, S. B. Lee, Y. K. H., J. Kim, J. K. Lim, N. Aratani, A. Tsuda, A. Osuka, and D. Kim, J. Am. Chem. Soc. **125**, 11062 (2003).
[34] C. Li, J. Ly, B. Lei, W. Fan, D. Zhang, J. Han, M. Mayyappan, C. Thompson, and M. Zhou, J. Phys. Chem. B **108**, 9646 (2004).
[35] M. P. Debreczeny, W. A. Svec, and M. R. Wasielewski, Science **274**, 584 (1996).
[36] T. van der Boom, R. T. Hayes, Y. Y. Zhao, P. J. Bushard, E. A. Weiss, and M. R. Wasielewski, J. Am. Chem. Soc. **124**, 9582 (2002).
[37] C. Liu, D. Walter, D. Neuhauser, and R. Baer, J. Am. Chem. Soc. **125**, 13936 (2003).
[38] Y. Imry and R. Landauer, Rev. Mod. Phys. **71**, S306 (1999).
[39] S. Datta, *Electronic Transport in Mesoscopic Systems* (Cambridge University Press, New York, 1995).
[40] M. P. Samanta, W. Tian, S. Datta, J. I. Henderson, and C. P. Kubiak, Phys. Rev. B **53**, R7626 (1996).
[41] S. N. Yaliraki, A. E. Roitberg, C. Gonzalez, V. Mujica, and M. A. Ratner, J. Chem. Phys. **111**, 6997 (1999).
[42] M. P. Lopez Sancho, J. M. L. Lopez Sancho, and J. Rubio, J. Phys. F: Met. Phys. **15**, 851 (1985).
[43] M. Di Ventra, S. T. Pantelides, and N. D. Lang, Phys. Rev. Lett. **84**, 979 (2000).
[44] Y. Xue, S. Datta, and M. A. Ratner, Chem. Phys. **281**, 151 (2002).
[45] A. Nitzan and M. A. Ratner, Science **300**, 1384 (2003).
[46] K. Stokbro, J. Taylor, M. Brandbyge, J. L. Mozos, and P. Ordejn, Comput. Mater. Sci. **27**, 151 (2002).
[47] A. D. Becke, J. Chem. Phys. **98**, 1372 (1993).
[48] A. D. Becke, J. Chem. Phys. **98**, 5648 (1993).
[49] W. R. Wadt and J. P. Hay, J. Chem. Phys. **82**, 299 (1985).
[50] Y. Shao, L. Fusti-Molnar, Y. Jung J. Kussmann *et al.*, Phys. Chem. Chem. Phys. **8**, 3172 (2006).
[51] M. F. Perutz, Annu. Rev. Biochem. **48**, 327 (1979).
[52] I. Schlichting, J. Berendzen, G. N. Phillips, and R. M. Sweet, Nature (London) **371**, 808 (1994).
[53] S. Franzen, L. Kiger, C. Poyart, and J.-L. Martin, Biophys. J. **80**, 2372 (2001).
[54] C. Rovira, K. Kunc, J. Hutter, P. Ballone, and M. Parrinello, J. Phys. Chem. A **101**, 8914 (1997).
[55] T. G. Spiro, P. M. Kozlowski, and M. Z. Zgierski, J. Raman Spectrosc. **29**, 869 (1998).
[56] J. M. Ugalde, B. Dunietz, A. Dreuw, M. Head-Gordon, and R. J. Boyd, J. Phys. Chem. A **108**, 4653 (2004).